Micromachines **2014**, *5*, 583-593; doi:10.3390/mi5030583

OPEN ACCESS

micromachines

ISSN 2072-666X

www.mdpi.com/journal/micromachines

Article

Inkjet Printing of High Aspect Ratio Superparamagnetic SU-8 Microstructures with Preferential Magnetic Directions

Loïc Jacot-Descombes [1,†,*], Maurizio R. Gullo [1,‡], Victor J. Cadarso [1,§], Massimo Mastrangeli [1,‖], Olgaç Ergeneman [2], Christian Peters [3], Philipe Fatio [2], Mouhamad A. Freidy [1], Christofer Hierold [3], Bradley J. Nelson [2] and Jürgen Brugger [1,*]

[1] Microsystems Laboratory, Ecole Polytechnique Fédérale de Lausanne (EPFL), 1015 Lausanne, Switzerland; E-Mails: g-mauri@iis.u-tokyo.ac.jp (M.R.G); victor.cadarso@psi.ch (V.J.C.); massimo.mastrangeli@ulb.ac.be (M.M.); m.freidy@rollomatic.ch (M.A.F)

[2] Multi-Scale Robotics Lab, Institute of Robotics and Intelligent Systems, ETH Zurich, 8092 Zurich, Switzerland; E-Mails: olgac.ergeneman@iris.mavt.ethz.ch (O.E.); fatiop@student.ethz.ch (P.F.); bnelson@ethz.ch (B.J.N)

[3] Micro and Nanosystems, ETH Zurich, 8092 Zurich, Switzerland; E-Mails: christian.peters@micro.mavt.ethz.ch (C.P.); christofer.hierold@micro.mavt.ethz.ch (C.H.)

† Present Address: Micro Resist Technology GmbH, Köpenicker Str. 325, 12555 Berlin, Germany.

‡ Present Address: Takeuchi Biohybrid System Laboratory, The University of Tokyo, Komaba, Tokyo 153-0041, Japan.

§ Present Address: Laboratory for Micro- and Nanotechnology, Paul Scherrer Institut, 5232 Villigen-PSI, Switzerland.

‖ Present Address: Bio, Electro and Mechanical Systems, Ecole Polytechnique, Université Libre de Bruxelles, 1050 Bruxelles, Belgium.

* Authors to whom correspondence should be addressed; E-Mails: l.jacot-descombes@microresist.de (L.J.); juergen.brugger@epfl.ch (J.B.); Tel.: +49-30-641-670-125 (L.J.); +41-21-693-6573 (J.B.).

Received: 29 June 2014; in revised form: 2 August 2014 / Accepted: 18 August 2014 / Published: 25 August 2014

Abstract: Structuring SU-8 based superparamagnetic polymer composite (SPMPC) containing Fe_3O_4 nanoparticles by photolithography is limited in thickness due to light absorption by the nanoparticles. Hence, obtaining thicker structures requires alternative processing techniques. This paper presents a method based on inkjet printing and thermal curing for the fabrication of much thicker hemispherical microstructures of SPMPC. The

microstructures are fabricated by inkjet printing the nanoparticle-doped SU-8 onto flat substrates functionalized to reduce the surface energy and thus the wetting. The thickness and the aspect ratio of the printed structures are further increased by printing the composite onto substrates with confinement pedestals. Fully crosslinked microstructures with a thickness up to 88.8 μm and edge angle of 112° ± 4° are obtained. Manipulation of the microstructures by an external field is enabled by creating lines of densely aggregated nanoparticles inside the composite. To this end, the printed microstructures are placed within an external magnetic field directly before crosslinking inducing the aggregation of dense Fe_3O_4 nanoparticle lines with in-plane and out-of-plane directions.

Keywords: inkjet printing; polymer; superparamagnetic SU-8; hemispherical structures; thermal curing; low topographical confinement; magnetic anisotropy

1. Introduction

In the last two decades, SU-8 has proven to be of great value for microelectromechanical systems (MEMS) fabrication thanks to its Young's modulus of 4.02 GPa, chemical and mechanical stability in addition to its simple wafer-scale processing, relatively low cost, and capability to reach high aspect ratio [1]. It has already been successfully used for a broad range of applications, such as among others, micro cantilevers [2], micro-optics [3], for microcapsule fabrication [4], as master for PDMS-based microfluidic setups [5], or as stamps for bio-medical purposes [6]. SU-8 and its derivatives can be prototyped by several methods, such as UV photolithography [7], two-photon polymerization [8], laser writing [9], inkjet printing (IJP) [10], or a combination of those technologies [11].

Furthermore, the possibility to remotely act on microsystems, such as by using external magnetic fields, shows a growing interest in various applications, for instance in-vivo medical devices, drug delivery or remote sensing [12]. The fabrication of magnetic microactuators by maskless photolithography based on photopolymer containing superparamagnetic nanoparticles (NP) has been recently demonstrated by Kim *et al.* [13]. Suter *et al.* have developed an SU-8-based superparamagnetic composite (SPMPC) containing Fe_3O_4 NP presented in [14] which enables actuation, shown by Ergeneman *et al.* [15], and compatible with both shadow-mask photolithography [16,17] and two-photon polymerization as shown Peters *et al.* [18].

Due to high absorption of the *i*-line radiation by the NP, the transmission of UV light inside the SPMPC is low, implying that its compatibility with photolithography is limited by the NP concentration and to layer thicknesses of few micrometers. This limit has been pushed further by Peters *et al.*, reaching slightly more than 10 μm with 5 vol % of NP using another photo initiator [19]. Alternatively, two-photon polymerization is well suited for multi-scale single structure prototyping but still time consuming for parallel large-scale manufacturing. As a solution, drop-on-demand (DOD) IJP of polymers as a fast prototyping method allows maskless fabrication of various shapes [20], among which hemispherical structures with enhanced profile. Confining the ink either by adjusting the surface energy or topographically by edge confinement enables targeting specific aspect ratios and high thicknesses [21–23]. Technically, confining a liquid drop by pinning its contact line on a convex edge

can be done with edges whose minimum heights are as low as the length range of the polymer chain [24,25]. Yet the confinement of inkjet printed micro drops has been so far described only on much higher pedestals, 5 μm [26]. Confinement on lower edges may be useful for a lot of applications, for example in micro-optics.

This paper presents the fabrication by DOD IJP of fully cured SU-8 based SPMPC microstructures (with 2 and 4 vol % of NP) by thermal crosslinking with high aspect ratio and thickness up to 88.8 μm. The microstructures are printed on flat glass substrates and on 1.0 ± 0.1 μm high pre-patterned confinement pedestals enabling increasing their heights and aspect ratio. Additionally, the printed structures are brought into an external magnetic field, before thermally crosslinking the composite, leading to preferential magnetic directions composed of dense NP lines. As an outcome of this work, these structures can be used after release from their substrates for instance for fluid-mediated self-organization or for directed self-assembly in an external magnetic field [27].

2. Experimental Section

2.1. Confinement Pedestals

The preparation of both substrates—flat and with the confinement pedestals—and their surface treatment is schematized in Figure 1a. The fabrication of the substrates with confinement pedestals starts with the cleaning and the surface activation of a purely amorphous SiO_2 wafer by a 4 min oxygen plasma (TePla 300, PVA TePla, Kirchheim bei München, Germay), Figure 1a$_1$. A 5 μm-thick layer of AZ9260 (from MicroChemicals) positive photoresist (PPR) is then spin-coated (EVG 150, EVG (Electronic Visions Group), St.Florian am Inn, Austria), followed by a 200 mJ/cm^2 exposure (Süss MA/BA6, SUSS MicroTec, Garching, Germany) and a development step (EVG 150). This results in a mask composed of protective PPR disks of 100 μm in diameter, Figure 1a$_2$. The SiO_2 is then etched for 8 min with reactive ion etching to pattern the substrate with the confining structures (Alcatel 601, Alcatel, Paris, France). The PPR is finally removed in a commercially available remover (SVC-14, Rohm and Haas, Philadelphia, PA, USA) and stripped by a 10-min oxygen plasma (Tepla 300), Figure 1a$_3$. In contrast, the flat substrates are microscope glass slides whose surface are also cleaned and activated by a 4-min oxygen plasma (Tepla 300), Figure 1a$_1$. Both substrates are finally silanized with Trichloro(1H,1H,2H,2H-perfluorooctyl)silanes (from Sigma Aldrich) in vapor phase in order to reduce their surface energy, Figure 1a$_4$.

The confinement pedestals, shown in Figure 1b, are fabricated by arrays of 10^4 on full 4″ wafers. One single wafer contains more than 10^5 100 μm pedestals with a pitch of 200 μm. Part of a pedestal array is shown by a scanning electron microscope (SEM) image in Figure 1b,c. The pedestal height has been measured with a mechanical profilometer and shows an average value of 1.0 ± 0.1 μm.

Figure 1. Substrate preparation: (**a**) fabrication schemes and (**b**,**c**) results. ($\mathbf{a}_{1,2}$) The substrate is coated with a positive photoresist (PPR) mask by photolithography, then ($\mathbf{a}_3$) etched and the PPR is stripped before ($\mathbf{a}_4$) the application of an anti-sticking layer. (**b**) Scanning electron microscope (SEM) side view image of a pedestal array and (**c**) zoom onto one circular pedestal with a diameter of 100 µm.

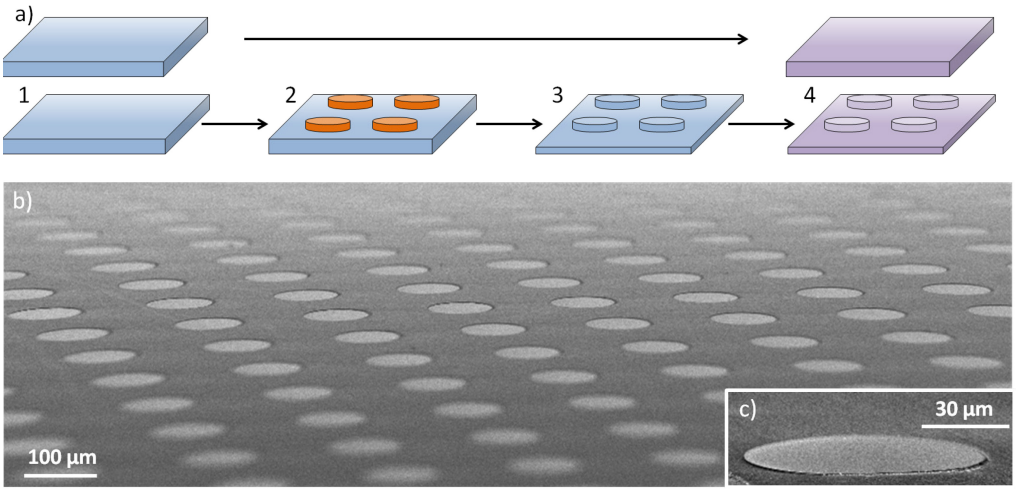

2.2. Experimental Setup

The experimental setup, installed in a yellow-light lab, is composed of a Microdrop DOD IJP station (Microdrop GmbH, Norderstedt, Germany) Newport motion stages (Newport Corporation, Irvine, CA, USA), and a custom made Helmholtz coil setup, Figure 2. The DOD IJP tool, as described in our previous work [23], makes use of a computer controlled piezo-actuated IJP head connected to the ink reservoir. The substrate is mounted onto the stage composed of two linear axes allowing printing onto defined locations. An additional rotational axis allows aligning the motions of the stage with the two main perpendicular directions of pre-patterned arrays.

2.3. Fabrication Process

The printing of microstructures is schematically shown in Figure 2a. Prior to printing, the SPMPC is diluted with gamma-Butyrolactone (GBL) and placed in ultrasonic bath for a minimum of 120 min to disperse the NP. For stable SPMPC drop generation, the DOD IJP head is operated at a voltage of 120 V, with a pulse length of 40 µs and a frequency of 100 Hz. The substrate is moved by the stages line by line producing a regular square array, Figure 2a. After the printing, the sample with non-crosslinked polymer containing the magnetic NP is positioned inside the Helmholtz coil setup where an external magnetic field of 8 mT is applied for 3 min. This allows aligning the NP into dense magnetic lines, as shown in Figure 2b. Based on the thermally-initiated crosslinking of SU-8 at temperatures > 137 °C and development not possible for soft-bake temperatures > 155 °C [28], a purely thermally induced crosslinking without photo-activation is performed by a bake of 3 h at 160 °C. This allows curing the structures and thus fixing the position and orientation of the magnetic lines within the polymer matrix, Figure 2c. The structures are then ready to be released, depending on the targeted application, as shown in Figure 2d.

Figure 2. Fabrication process: (**a**) inkjet printing (IJP) of the SPMPC (**b**) exposure of uncured superparamagnetic polymer composite (SPMPC) to an external magnetic field provided by a Helmholtz coil setup (**c**) curing of the printed structures at 160 °C for 3 h in the oven (**d**) final structures with programmed preferential magnetic directions.

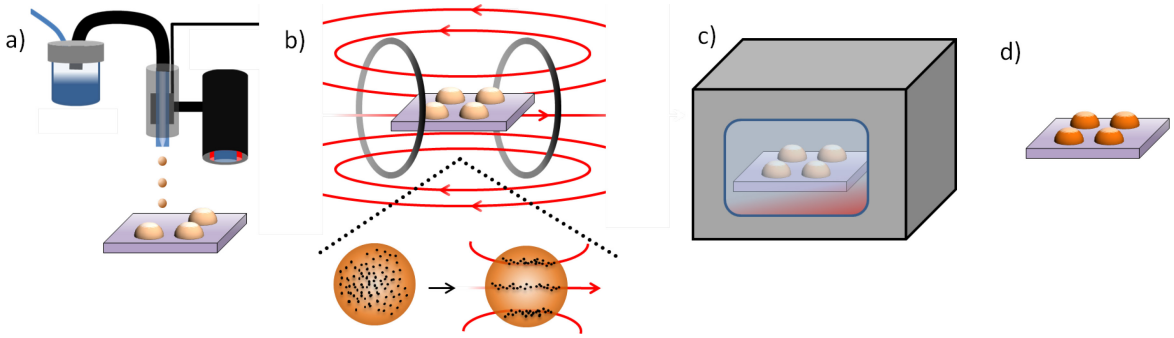

3. Results and Discussions

3.1. Inkjet Printed Structures on Flat Substrates

The SPMPC has been first printed in the form of droplets onto the flat substrates, leading to spherical cap shapes. This approach has still three limitations: (1) each specific surface treatment leads to a specific spherical cap shape, which cannot be changed. An example of contact angle is shown in Figure 3b with a drop printed on a silanized flat substrate having typical contact angle of 46.5° giving an aspect ratio of 0.21. (2) The structure alignment within an array is mainly limited by the reproducibility of the generated drop direction when ejected from the nozzle. An example of a resulting misalignment is shown in the printed array of Figure 3c where structures of 130 µm in diameter deviate locally by few tens of micrometers. (3) The withdrawal of the printed drop—due to the volume shrinkage—occurring during the solvent evaporation and the crosslinking is not controlled leading to asymmetric structures and increasing the final misalignment. This withdrawal is nicely shown by the 10 µm-long NP agglomerates' traces left on the substrate after receding, Figure 3d.

Figure 3. Inkjet printed spherical structures onto silanized flat substrate (**a**) schematics and (**b**) SEM side view of a printed drop with a typical contact angle after curing of 46.5°. (**c**) Top view optical images showing a printed array; their misalignment—resulting from their random pinning line receding—is highlighted by the white straight lines, and the crosses point out the misaligned structures. (**d**) Top view SEM images of the edge of one printed structure and zoom showing traces of nanoparticle (NP) agglomerates (on silicon substrate for imaging reasons with the same surface coating).

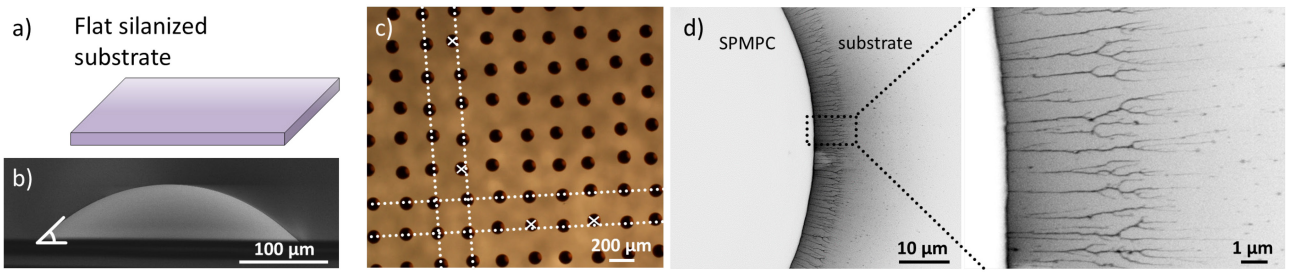

3.2. High Aspect Ratio Structures on Confinement Pedestals

In order to increase the height of the crosslinked SPMPC structures by increasing and selecting their final edge angle [23] and to overcome the three limitations discussed, the printing has been performed onto pedestals. Indeed, the pre-patterned confinement pedestals are defining the final contour of the structures controlling the evolution of edge angle and diameter during the volume loss, Figure 4a,b. A complete study of these evolutions has been presented in our previous work [23] and by Chen *et al.* [20,29]. Finally, the eventual misalignment within an array is solved by the self-centering of the drops onto the pre-pattered pedestals (Figure 4c), so that the position accuracy of the structures is given by the one of the pedestals. If large enough volume has been deposited, during curing the volume reduction implies mainly a height reduction and negligible reduction of the diameter of the spherical cap base. As a consequence, there is almost no recession for a drop covering the complete pedestal, as shown with the three isolated microstructures in the SEM side view image of Figure 4d. No recession implies preservation of the diameter and no traces left around the microstructures. The structures shown in Figure 4 are confined on 1.0 ± 0.1 µm high and 100 µm in diameter glass platforms. Aspect ratios up to 0.7 can be measured, with a height up to 88.8 µm and a maximum diameter of 125.6 µm. As expected, the structures follow a hemispherical cap profile. The low height of the confinement platforms is clearly demonstrated on the SEM image of Figure 4d, where a specific case of a platform of 850 nm in height is shown.

Figure 4. Printed SPMPC spherical structures on confining pedestals (**a**) substrate scheme and (**b**) side view SEM image showing edge angles of 112° ± 4°. (**c**) Top view optical image of a 5 by 5 array printed on pedestals next to a 10-cents Swiss coin and inset of the array, showing the well aligned microstructures. (**d**) SEM side view image showing three isolated spherical structures and zoom into one confinement pedestal with the printed structure; this specific example has a height of 850 nm, but the average height has been measured at 1.0 ± 0.1 µm.

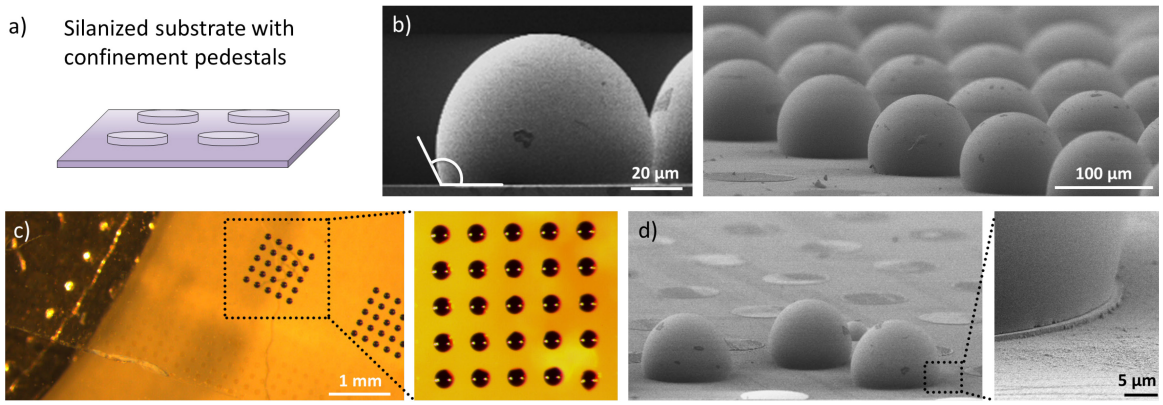

3.3. Induced Preferential Magnetic Directions

Dense magnetic lines are induced into the inkjet printed structures by introducing them into a magnetic field (Figure 1b–d) directly after printing. The time frame for this transition is critical. Indeed, the solvents evaporate increasing the viscosity and decreasing the mobility of the NP. In order

to evaluate the time window, an array of 20 × 20 hemispheres with a time shift of 1.45 s between each structure was printed. Figure 5 shows selected structures of this array. The structures are numbered in the array following their position. Structure #1 is the last that was printed, thus having the shortest time shift between printing and applying the magnetic field. The higher the number is, the longer the delay between printing and exposure to field. The transfer from the inkjet station into the magnetic setup took 30 s. It can be discerned from Figure 5 that after the structure #55 the magnetic field was not able to align the NP in the SPMPC any longer. This corresponds to a maximum print time of 2 min before applying the magnetic field. This time window can be controlled as presented below. This limits the number of printed structures with magnetic lines.

The crosslinking of the structures is performed by a bake of 3 h at 160 °C. However, during the baking before the composite starts crosslinking, the SPMPC reflows although the samples are brought directly to 160 °C with no ramp. As a first consequence, a fraction of the particle alignment is lost but no influence on the Fe_3O_4 NP properties is expected [30]. This particle alignment reduction is revealed by the slight blurring of the lines visible in Figure 6a showing the same microstructure before (Figure 6a upper image) and after curing (Figure 6a lower image). A possible setup improvement allowing reducing this effect is described below. In addition, the thermal reflow also induces a 20% reduction of the structure diameter, as well revealed in Figure 6a. The contour of the structure which is slightly asymmetric before curing—resulting from the solvent evaporation and pinning on substrate—becomes round again. Nevertheless, the shape of the printed structure can be well controlled, as presented above and described in [23].

Based on this approach, microstructures with either in-plane or out-of-plane magnetic lines have been fabricated. Figure 6b–d shows microstructures with diameters of 250 µm without as reference (Figure 6b), with in-plane (Figure 6c) and with out-of-plane (Figure 6d) magnetic lines.

Figure 5. Optical micrographs of the central part of some individual microstructures in a 20 × 20 printed array. The positions of the structures within the array are given by the numbers. The scale bar is 50 µm.

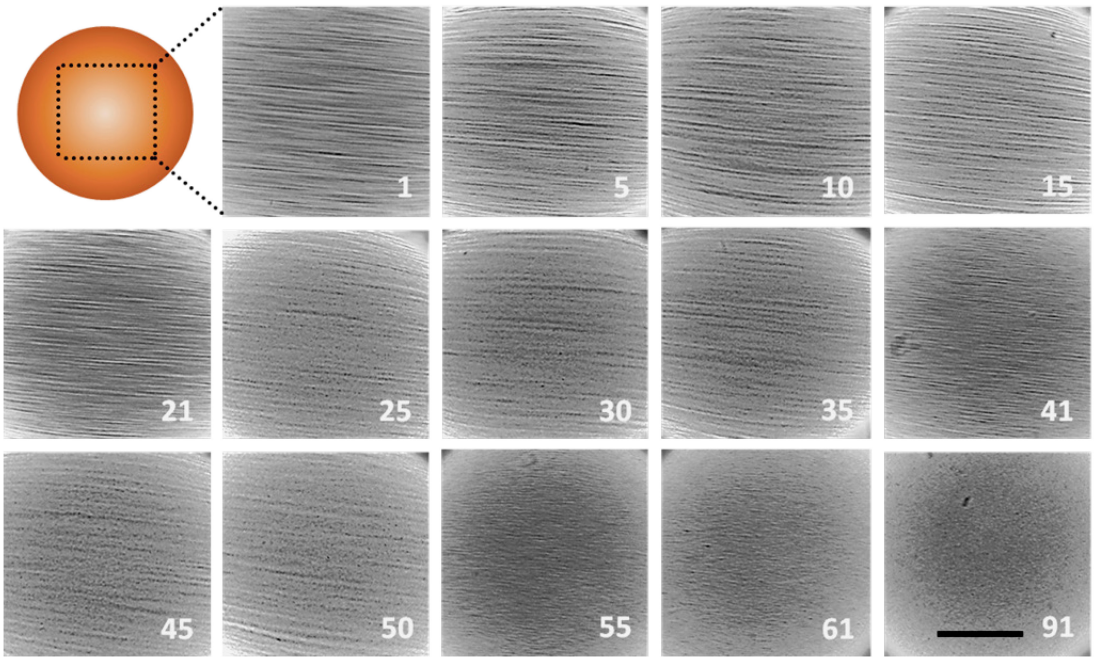

Figure 6. (**a**) Optical top view images of a printed structure before (upper image) and after (lower image) thermal curing at 160 °C. Schemes of the field application and associated top view optical images of the central part of the structures (**b**) without, (**c**) with in-plane and (**d**) with out of plane magnetic lines. The scale bar is 50 µm.

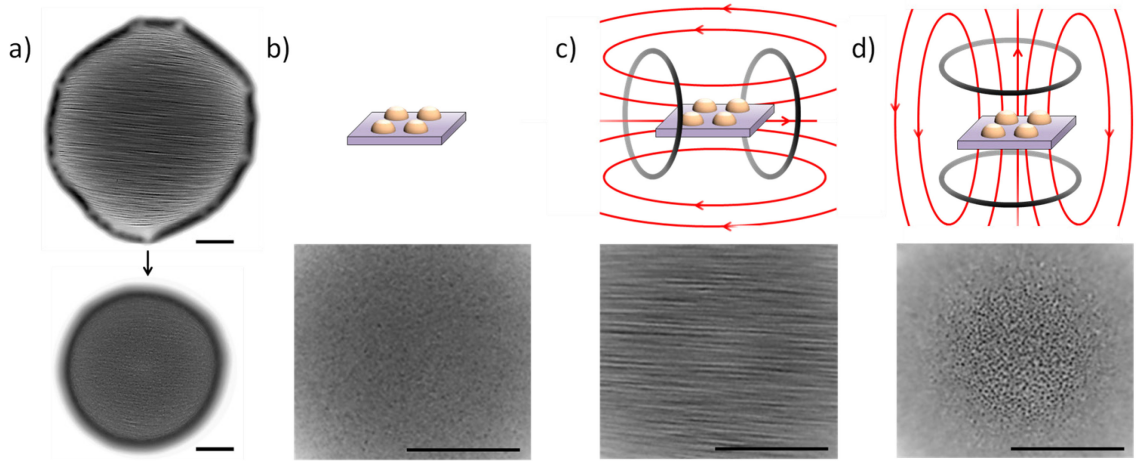

3.4. Further Discussions and Improvements

There are still two limitations, (1) the throughput of this fabrication approach and (2) the reduction of preferential magnetic directions during the thermal curing. The throughput is mainly limited by the short-time window allowing the rearrangement of the NP while applying the magnetic field. As a possible improvement, we foresee a setup improvement where all components—the inkjet printing station, the magnetic setup and a hotplate for the curing of the structures—are combined together. Through this approach, the magnetic lines could be induced into the complete printed arrays and maintained by the magnetic field during the thermal curing. The overall throughput of the proposed method and the preferential magnetic directions would be enhanced.

4. Conclusions

The drop-on-demand inkjet printing of superparamagnetic polymer composite containing Fe_3O_4 nanoparticles has been demonstrated for the fabrication of spherical cap structures onto flat and pre-patterned glass substrates. By successfully confining the structures onto 1 µm high and 100 µm wide pedestals their aspect ratio was increased by up to more than 3 times as compared to its value on flat substrates. Thicknesses up to 88.8 µm of fully crosslinked structures were reached. The low UV transmission prohibiting photo-curing such thick structures was solved by thermally curing the printed structures.

In a second phase, the printed structures were brought into an external magnetic field prior to curing in order to rearrange the Fe_3O_4 NP into dense magnetic lines. Between inkjet printing and application of the magnetic field, a maximum time window of 2 min was determined. Structures with in-plane and out-of-plane magnetic dense lines were fabricated, leading to an anisotropic magnetic behavior once brought into external magnetic fields. A targeted application is the remote control by magnetic actuation of the free floating microstructures—after release from their substrate—in view of their controlled fluid-mediated self-assembly.

Acknowledgments

The authors would like to express their great thanks to the CMi staff for their precious help during the preparation of the substrates as well as to Ikjoo Byun from the group of Beomjoon Kim for early experimental work. This work has been scientifically evaluated by SNSF as well as funded by the Swiss National Science Foundation via the Nano-Tera.ch program.

Author Contributions

Loïc Jacot-Descombes and Maurizio R. Gullo contributed equally to this work. Loïc Jacot-Descombes wrote the main part of the paper and mainly conducted the inkjet printing experiments during the first phase, done as well with Mouhamad A. Freidy. During the second phase, Victor J. Cadarso mainly conducted the inkjet printing experiments. Maurizio R. Gullo planned the overall collaboration and experimental work, as well as took part during all experimental work and wrote a significant part of the manuscript. Massimo Mastrangeli supported the inkjet printing experiments, gave scientific understanding on liquid confinement and reviewed the manuscript. Olgaç Ergeneman initiated the work bringing in the key idea and conducted as well the second phase of the experiments involving the magnetic field setup. Philipe Fatio and Christian Peters took part in the magnetic field actuation and dense magnetic line generation. Christofer Hierold, Bradley J. Nelson and Jürgen Brugger supervised the work and reviewed the manuscript.

Conflicts of Interest

The authors declare no conflict of interest.

References

1. Lorenz, H.; Despont, M.; Fahrni, N.; LaBianca, N.; Renaud, P.; Vettiger, P. SU-8: A low-cost negative resist for MEMS. *J. Micromech. Microeng.* **1997**, *7*, 121–124.
2. Genolet, G.; Brugger, J.; Despont, M.; Drechsler, U.; Vettiger, P.; de Rooij, N.F.; Anselmetti, D. Soft, entirely photoplastic probes for scanning force microscopy. *Rev. Sci. Instrum.* **1999**, *70*, 2398–2401.
3. Voigt, A.; Ostrzinski, U.; Pfeiffer, K.; Kim, J.Y.; Fakhfouri, V.; Brugger, J.; Gruetzner, G. New inks for the direct drop-on-demand fabrication of polymer lenses. *Microelectron. Eng.* **2011**, *88*, 2174–2179.
4. Jacot-Descombes, L.; Martin-Olmos, C.; Gullo, M.R.; Cadarso, V.J.; Mermoud, G.; Villanueva, L.G.; Mastrangeli, M.; Martinoli, A.; Brugger, J. Fluid-mediated parallel self-assembly of polymeric micro-capsules for liquid encapsulation and release. *Soft Matter* **2013**, *9*, 9931–9938.
5. McDonald, J.C.; Duffy, D.C.; Anderson, J.R.; Chiu, D.T.; Wu, H.K.; Schueller, O.J.A.; Whitesides, G.M. Fabrication of microfluidic systems in poly(dimethylsiloxane). *Electrophoresis* **2000**, *21*, 27–40.
6. Nagstrup, J.; Keller, S.; Almdal, K.; Boisen, A. 3D microstructuring of biodegradable polymers. *Microelectron. Eng.* **2011**, *88*, 2342–2344.

7. Lorenz, H.; Despont, M.; Fahrni, N.; Brugger, J.; Vettiger, P.; Renaud, P. High-aspect-ratio, ultrathick, negative-tone near-UV photoresist and its applications for MEMS RID C-5357-2009 RID A-6994-2011. *Sens. Actuators Phys.* **1998**, *64*, 33–39.
8. Suter, M.; Zhang, L.; Siringil, E.C.; Peters, C.; Luehmann, T.; Ergeneman, O.; Peyer, K.E.; Nelson, B.J.; Hierold, C. Superparamagnetic microrobots: fabrication by two-photon polymerization and biocompatibility. *Biomed. Microdevices* **2013**, *15*, 997–1003.
9. Cadarso, V.J.; Pfeiffer, K.; Ostrzinski, U.; Bureau, J.B.; Racine, G.A.; Voigt, A.; Gruetzner, G.; Brugger, J. Direct writing laser of high aspect ratio epoxy microstructures. *J. Micromech. Microeng.* **2011**, *21*, 017003.
10. Fakhfouri, V.; Cantale, N.; Mermoud, G.; Kim, J.Y.; Boiko, D.; Charbon, E.; Martinoli, A.; Brugger, J. Inkjet printing of SU-8 for polymer-based MEMS a case study for microlenses. In Proceedings of IEEE 21st International Conference on Micro Electro Mechanical Systems, Tucson, AZ, USA, 13–17 January 2008; pp. 407–410.
11. Cadarso, V.J.; Smolik, G.; Auzelyte, V.; Jacot-Descombes, L.; Brugger, J. Heterogeneous material micro-transfer by ink-jet print assisted mould filling. *Microelectron. Eng.* **2012**, *98*, 619–622.
12. Nelson, B.J.; Kaliakatsos, I.K.; Abbott, J.J. Microrobots for Minimally Invasive Medicine. *Annu. Rev. Biomed. Eng.* **2010**, *12*, 55–85.
13. Kim, J.; Chung, S.E.; Choi, S.-E.; Lee, H.; Kim, J.; Kwon, S. Programming magnetic anisotropy in polymeric microactuators. *Nat Mater* **2011**, *10*, 747–752.
14. Suter, M.; Graf, S.; Ergeneman, O.; Schmid, S.; Camenzind, A.; Nelson, B.J.; Hierold, C. Superparamagnetic photosensitive polymer nanocomposite for microactuators. In Proceedings of Solid-State Sensors, Actuators and Microsystems Conference, Denver, CO, USA, 21–25 June 2009; pp. 869–872.
15. Ergeneman, O.; Suter, M.; Chatzipirpiridis, G.; Zurcher, J.; Graf, S.; Pane, S.; Hierold, C.; Nelson, B.J. Characterization and actuation of a magnetic photosensitive polymer cantilever. In Proceedings of International Symposium on Optomechatronic Technologies, Istanbul, Turkey, 21–23 September 2009; pp. 266–270.
16. Suter, M.; Ergeneman, O.; Zürcher, J.; Moitzi, C.; Pané, S.; Rudin, T.; Pratsinis, S.E.; Nelson, B.J.; Hierold, C. A photopatternable superparamagnetic nanocomposite: Material characterization and fabrication of microstructures. *Sens. Actuators B Chem.* **2011**, *156*, 433–443.
17. Suter, M.; Ergeneman, O.; Zürcher, J.; Schmid, S.; Camenzind, A.; Nelson, B.J.; Hierold, C. Superparamagnetic photocurable nanocomposite for the fabrication of microcantilevers. *J. Micromech. Microeng.* **2011**, *21*, 025023.
18. Peters, C.; Ergeneman, O.; García, P.D.W.; Müller, M.; Pané, S.; Nelson, B.J.; Hierold, C. Superparamagnetic twist-type actuators with shape-independent magnetic properties and surface functionalization for advanced biomedical applications. *Adv. Funct. Mater.* **2014**, doi:10.1002/adfm.201400596.
19. Peters, C.; Ergeneman, O.; Sotiriou, G.A.; Pratsinis, S.E.; Nelson, B.J.; Hierold, C. Pushing the limits of photo-curable SU-8-based superparamagnetic polymer composites. In Proceedings of 2013 Transducers Eurosensors XXVII: The 17th International Conference on Solid-State Sensors, Actuators and Microsystems, Barcelona, Spain, 16–20 June 2013; pp. 2676–2679.

20. Chen, C.-T.; Chiu, C.-L.; Hsu, C.-Y.; Tseng, Z.-F.; Chuang, C.-T. Inkjet-Printed Polymeric Microstructures in n-Sided Regular Polygonal Cavities. *J. Microelectromech. Syst.* **2011**, *20*, 1001–1009.
21. Lu, J.-P.; Huang, W.-K.; Chen, F.-C. Self-positioning microlens arrays prepared using ink-jet printing. *Opt. Eng.* **2009**, *48*, 073606.
22. Chen, C.-T.; Tseng, Z.-F.; Chiu, C.-L.; Hsu, C.-Y.; Chuang, C.-T. Self-aligned hemispherical formation of microlenses from colloidal droplets on heterogeneous surfaces. *J. Micromech. Microeng.* **2009**, *19*, 025002.
23. Jacot-Descombes, L.; Gullo, M.R.; Cadarso, V.J.; Brugger, J. Fabrication of epoxy spherical microstructures by controlled drop-on-demand inkjet printing. *J. Micromech. Microeng.* **2012**, *22*, 074012.
24. Ondarcuhu, T.; Piednoir, A. Pinning of a contact line on nanometric steps during the dewetting of a terraced substrate. *Nano Lett.* **2005**, *5*, 1744–1750.
25. Chang, B.; Shah, A.; Routa, I.; Lipsanen, H.; Zhou, Q. Low-height sharp edged patterns for capillary self-alignment assisted hybrid microassembly. *J. Micro-Bio Robot.* **2014**, *9*, 1–10.
26. Jacot-Descombes, L.; Gullo, M.R.; Mastrangeli, M.; Cadarso, V.J.; Brugger, J. Inkjet printed SU-8 hemispherical microcapsules and silicon chip embedding. *Micro Nano Lett.* **2013**, *8*, 633–636.
27. Ergeneman, O.; Peters, C.; Gullo, M.R.; Jacot-Descombes, L.; Gervasoni, S.; Özkale, B.; Fatio, P.; Cadarso, V.J.; Mastrangeli, M.; Pané, S.; Brugger, J.; Hierold, C.; Nelson, B. Inkjet printed superparamagnetic polymer composite hemispheres with programmed magnetic anisotropy. *Nanoscale* **2014**, doi:10.1039/C3NR06442E.
28. Ong, B.H.; Yuan, X.; Tao, S.; Tjin, S.C. Photothermally enabled lithography for refractive-index modulation in SU-8 photoresist. *Opt. Lett.* **2006**, *31*, 1367–1369.
29. Chen, C.-T.; Tu, K.-Z. Inkjet printing of individual polymer micro parts self-shaped with hemispherical caps. *Sens. Actuators Phys.* **2011**, *188*, 367–373.
30. Gao, M. Synthesis and Characterization of superparamagnetic Fe_3O_4@SiO_2 core-shell composite nanoparticles. *World J. Condens. Matter Phys.* **2011**, *1*, 49–54.